

Effects of Host–Guest Recognition on Kinetics of Diels–Alder Reaction of Quinocrown Ethers with Cyclopentadiene

Akihiko Tsuda[†] and Takumi Oshima*

Department of Applied Chemistry, Faculty of Engineering, Osaka University,
Machikaneyama 1-16, Toyonaka, Osaka 560-0043, Japan

oshima@ch.wani.osaka-u.ac.jp

Received October 10, 2001

Diels–Alder reactions of 15–21-membered quinocrown ethers **1a–c** and 18-membered quinobenzocrown ether **1d** with cyclopentadiene were catalyzed by the addition of alkali, alkaline earth metal and ammonium perchlorates, and scandium trifluoromethane-sulfonate. The alkali metal and ammonium ions brought about a fairly selective rate-acceleration for each crown ether due to the size-fitted *ion-in-the-hole* complexation. However, such a hole-size-selectivity was not observed for the reactions catalyzed by divalent alkaline-earth (Mg^{2+} to Ba^{2+}) and trivalent Sc^{3+} ions. The *wrapping* complexation played a significant role in rate-acceleration in such a way that the smallest Mg^{2+} caused 160 times rate-enhancement for the most flexible **1c** and the Sc^{3+} performed maximal 3700 times rate-increment for the 18-membered quinobenzocrown **1d**. These effects of cation recognition were rationalized by the reduction of LUMO energy that is favored by the orbital interaction with the HOMO of cyclopentadiene. The magnitude of rate-enhancement was discussed in terms of the cation binding affinity and coordination geometry of quinocrown ethers as well as the valence of cations.

Introduction

Since the discovery of crown ethers by Pedersen in 1967,¹ a large number of host–guest complexes using ion–dipole interactions have been reported.² Their elegant supramolecular structure and functionality both in solution and the crystal state have attracted much interest in light of their applications for material science and recently advanced nanoscale technology.³ However, there are only a limited number of reports on the study of reaction control by such host–guest complexation in a biomimetic manner.⁴ In this context, we focused on the effects of guest recognitions on the reactivity of supramolecules by using selective cation binding behavior of crown ethers.

Herein, we present a systematic study of the effects of cation recognition on the kinetics of Diels–Alder reactions of 15–21 membered ring quinocrown ethers **1a–d** (quino[15]crown-5 **1a**, quino[18]crown-6 **1b**, quino[21]crown-7 **1c**, quinobenzo[18]crown-6 **1d**) with cyclopentadiene in comparison with the reaction of 2,3-dimethoxy-1,4-benzoquinone **2** as a reference compound. These quinocrown ethers are ditopic host molecules which introduced an electron-accepting quinone moiety to macrocyclic polyether linkage, and **1a,b** are also known to react with cyclopentadiene at the outer C=C double bond to give the [4 + 2] *endo* adducts in 92–98% yield as represented for **1b** (Scheme 1).⁵ We expected that the cycloadditions of quinocrown ethers with cyclopentadiene are effectively catalyzed by the incorporation of a guest cation as the Lewis acid into the crown ether linkage, and the binding features for the various combinations of host and guest must be reflected on the magnitude of rate-acceleration. This principle can be readily envisaged

* Corresponding author. Fax: +81-6-6850-5785. E-mail: oshima@ch.wani.osaka-u.ac.jp.

[†] Current address: Department of Chemistry, Graduate School of Science, Kyoto University, Sakyo-ku, Kyoto 606-8502, Japan.

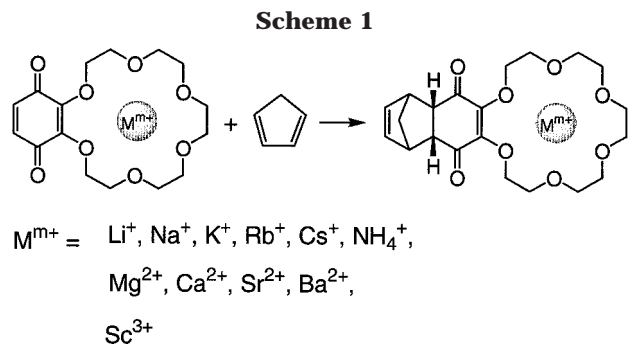
(1) (a) Pedersen, C. J. *J. Am. Chem. Soc.* **1967**, *89*, 2495. (b) Pedersen, C. J. *J. Am. Chem. Soc.* **1967**, *89*, 7017. (c) Pedersen, C. J.; Frensdorff, H. K. *Angew. Chem., Int. Ed. Engl.* **1972**, *11*, 16.

(2) (a) Lehn, J.-M. *Science* **1985**, *227*, 849. (b) Inoue, Y.; Gokel, G. W. *Cation Binding by Macrocycles*, Marcel Dekker: New York, 1990. (c) Echevoyen, L. E.; Yoo, H. K.; Gatto, V. J.; Gokel, G. W.; Echevoyen, L. *J. Am. Chem. Soc.* **1989**, *111*, 2440. (d) Lehn, J.-M. *Supramolecular Chemistry*, Verlags: Weinheim, 1995. (e) Yaghi, O. M.; Li, G.; Li, H. *Nature* **1995**, *378*, 703. (f) Kang, J.; Rebeck, J., Jr. *Nature* **1996**, *382*, 239. (g) Wolbers, M. P. O.; Veggel, C. J. M.; Snellink-Ruel, B. H. M.; Hofstra, J. W.; Geurts, F. A. J.; Reinhoubt, D. N. *J. Am. Chem. Soc.* **1997**, *119*, 138. (h) Ballardini, R.; Balazani, V.; Credi, A.; Brown, C. L.; Gillard, R. E.; Montalti, M.; Philp, D.; Stoddard, J. F.; Venturi, M.; White, A. J. P.; Williams, B. J.; Williams, D. J. *J. Am. Chem. Soc.* **1997**, *119*, 12503. (i) Ikeda, A.; Shinkai, S. *Chem. Rev.* **1997**, *97*, 1713. (j) Kobayashi, K.; Koyanagi, M.; Endo, K.; Masuda, H.; Aoyama, Y. *Chem. Eur. J.* **1998**, *4*, 417. (k) Meadoes, E. S.; Wall, S. L. D.; Barbour, L. J.; Fronczek, F. R.; Kim, M.-S.; Gokel, G. W. *J. Am. Chem. Soc.* **2000**, *122*, 3325.

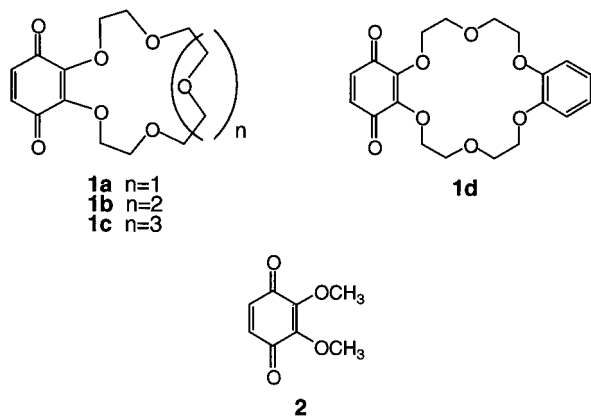
(3) Balzani, V.; Credi, A.; Raymo, F. M.; Stoddart, J. F. *Angew. Chem., Int. Ed.* **2000**, *39*, 3348.

(4) (a) Gold, V.; Sghibartz, C. M. *J. Chem. Soc., Chem. Commun.* **1978**, 507. (b) Inoue, Y.; Ouchi, M.; Hayama, H.; Hakushi, T. *Chem. Lett.* **1983**, 431. (c) Cacciapaglia, R.; Lucente, S.; Mandolini, L. *Tetrahedron* **1989**, *45*, 5293. (d) Oshima, T.; Nagai, T. *J. Org. Chem.* **1991**, *56*, 673. (e) Cacciapaglia, R.; Doorn, A. R.; Mandolina, L.; Reinhoudt, D. N.; Verboon, W. *J. Am. Chem. Soc.* **1992**, *114*, 2611. (f) Gobbi, A.; Landini, D.; Maria, A.; Secci, D. *J. Org. Chem.* **1995**, *60*, 5954. (g) Gobbi, A.; Landini, D.; Maria, A.; Penso, M. *J. Chem. Soc., Perkin Trans. 2* **1996**, 2505. (h) Cacciapaglia, R.; Mandolini, L.; Arnecke, R.; Böhmer, V.; Vogt, W. *J. Chem. Soc., Perkin Trans. 2* **1998**, 419. (i) Brrecia, P.; Cacciapaglia, R.; Mandolini, L.; Scorsini, C. *J. Chem. Soc., Perkin Trans. 2* **1998**, 1257. (j) Kang, J.; Santamaria, J.; Hilmersson, G.; Rebeck, J., Jr. *Rebeck, J. Am. Chem. Soc.* **1998**, *120*, 3650. (k) Kang, J.; Santamaria, J.; Hilmersson, G.; Rebeck, J., Jr. *J. Am. Chem. Soc.* **1998**, *120*, 7389. (l) Tsuda, A.; Oshima, T. *New J. Chem.* **1998**, 1027. (m) Itoh, S.; Taniguchi, M.; Takada, N.; Nagatomo, S.; Kitagawa, T.; Fukuzumi, S. *J. Am. Chem. Soc.* **2000**, *122*, 12087.

(5) (a) Dietl, F.; Gierer, G.; Merz, A. *Synthesis* **1985**, 626. (b) Hayakawa, K.; Kido, K.; Kanematu, K. *J. Chem. Soc., Perkin Trans. 1* **1988**, 511.

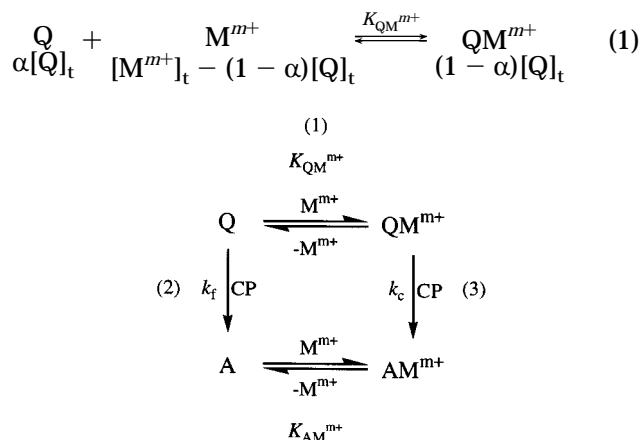


by considering that the guest cations lower the LUMO energy against the HOMO of cyclopentadiene, thus enhancing the FMO interaction.⁶



Results and Discussion

Complex Formation and Treatment of Kinetic Data. The [4 + 2] cycloadditions of quinocrown ethers (Q) and cyclopentadiene (CP) in the presence of metal ions (M^{m+}) can be envisaged as given in eqs 1–3. In eq 1, the metal ion is able to form a 1:1 complex with Q, where the reaction 1 is at rapid equilibrium, binding constant $K_{QM^{m+}}$. The $[Q]_t$ and $[M^{m+}]_t$ are the total concentrations of Q and M^{m+} , respectively. The produced [4 + 2] adducts (A) may have little effect on binding constants ($K_{QM^{m+}} \approx K_{AM^{m+}}$), since the observed pseudo-first-order rate constants were not affected during the reactions by their adduct formation even at the various concentration of metal ions (an excellent correlation coefficient is always attained $r > 0.999$).



The [4 + 2] adducts were formed from free Q (eq 2) and the cation complexed QM^{m+} (eq 3), with the rate

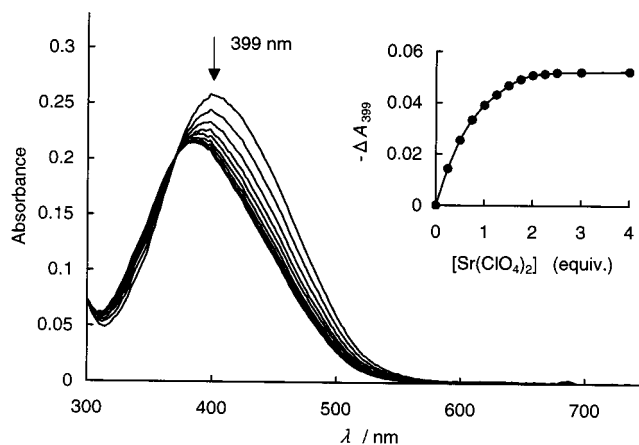


Figure 1. Absorption spectra of quino[15]crown-5 **1a** (0.20 mM) in MeCN solution at variable concentrations of $\text{Sr}(\text{ClO}_4)_2$ (0 to 0.40 mM) at 298 K. Inset: Correlation of absorbance decrease ($-\Delta A_{399}$) at 399 nm of the quino[15]crown-5 **1a** with concentration of $\text{Sr}(\text{ClO}_4)_2$. The $-\Delta A_{399}$ are plotted against molar equivalents of added salt.

constants k_f and k_c , respectively. In eq 1, the binding constant $K_{QM^{m+}}$ is defined by

$$K_{QM^{m+}} = [QM^{m+}]/[Q][M^{m+}] = (1 - \alpha)/\alpha[M^{m+}] \quad (4)$$

The observed rate constant k_{obsd} is given as

$$k_{\text{obsd}} = \alpha k_f + (1 - \alpha)k_c \quad (5)$$

The values of $K_{QM^{m+}}$ for complexation of Q with M^{m+} were obtained by titration experiments using the UV–visible spectroscopic changes due to complexation of these components.⁷ The titration profile of a typical decreasing absorption change by addition of $\text{Sr}(\text{ClO}_4)_2$ into the MeCN solution containing quino[15]crown-5 **1a** (0.20 mM) at 298 K is shown in Figure 1 along with the plot of differential absorbance, $-\Delta A = A_{\text{obsd}} - A_f$, at $\lambda_{\text{max}} = 399$ nm against the metal concentration, where A_f is the initial absorbance of free **1a** and A_{obsd} is the absorbance in the presence of metal salt. The $K_{QM^{m+}}$ were determined as follows. The A_c values were estimated from the A_{obsd} at the point of large excess of $[M^{m+}]_t$ to $[Q]_t$, where A_c is the absorbance of complexed quinocrown ether. Under these conditions, $[QM^{m+}]$ attains saturation; thus A_{obsd} can be regarded as A_c . Using this A_c value, the $K_{QM^{m+}}$ values in eq 6 is calculated, and the reasonably reliable values of A_c and $K_{QM^{m+}}$ are also obtainable by nonlinear least-squares curve-fitting analysis.⁸ Equation 6 is introduced by eq 5 and eq 4, and by alternation of the rate constant k to the absorbance A .

$$K_{QM^{m+}} = (A_f - A_{\text{obsd}})/(A_{\text{obsd}} - A_c)[M^{m+}] \quad (6)$$

where

$$[M^{m+}] = [M^{m+}]_t - [Q]_t(A_f - A_{\text{obsd}})/(A_f - A_c) \quad (7)$$

(6) (a) Woodward, R. B.; Hoffmann, R. *Angew. Chem.* **1969**, *81*, 797. (b) Fleming, I. *Frontier Orbitals and Organic Chemical Reactions*; John Wiley: London, 1976.

(7) The monitored wavelength at λ_{max} (e) is as follows: **1a** ($\lambda_{\text{max}} = 399$ nm, $\epsilon = 131 \text{ M}^{-1} \text{ cm}^{-1}$), **1b** (399, 129), **1c** (399, 130), **1d** (399, 130), **2** (391, 104).

Table 1. Alkali Metal and Ammonium Ion Catalyzed Diels–Alder Reactions of Quinones **1a–d** and **2** with Cyclopentadiene in MeCN at 30 °C^a

quinone(Q)	10 ² <i>k_f</i> M ⁻¹ s ⁻¹	<i>k_{obsd}</i> / <i>k_f</i> ^b for each additive ^c					
		Li ⁺	Na ⁺	K ⁺	Rb ⁺	Cs ⁺	NH ₄ ⁺
1a	5.23	2.14	2.66	3.71	1.50	1.32	1.41
1b	4.60	1.45	1.98	3.72	2.98	2.08	2.80
1c	4.76	1.72	1.53	1.74	2.48	2.58	2.18
1d	5.31	1.41	1.92	2.32	1.94	1.31	1.75
2	5.33	1.03	1.00	1.04	1.04	1.02	1.07

^a Kinetic reactions were carried out under pseudo-first-order conditions by using an excess of cyclopentadiene (16.0 mM) with respect to quinones **1** and **2** (0.167 mM). The observed second-order rate constants *k_{obsd}* were the average of at least two measurements. Error limit of the *k_{obsd}* is ±2%. ^b The *k_f* values are taken from the salt-free reactions. ^c The 24 equiv excess of alkali metal or ammonium perchlorate (4.0 mM) with respect to quinones was used. Counteranion perchlorate (ClO₄⁻) is omitted.

On the other hand, under the Benesi–Hildebrand conditions ($[M^{m+}]_t/[Q]_t \geq 10$), *A_{obsd}* and $[M^{m+}]_t$ are correlated as shown in eq 8, where $\Delta A_{obsd} = A_{obsd} - A_f$ and $\Delta A_c = A_c - A_f$.⁹ Plots of $1/\Delta A_{obsd}$ vs $1/[M^{m+}]_t$ give a straight line, and the two unknowns, *K_{QM^{m+}}* and ΔA_c , are obtained from the slope and intercept, respectively.

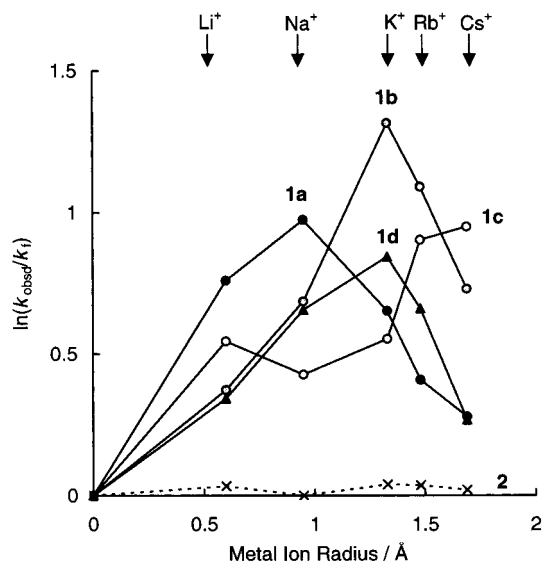
$$1/\Delta A_{obsd} = 1/\Delta A_c + 1/K_{QM}^{m+} \times 1/\Delta A_c \times 1/[M^{m+}]_t \quad (8)$$

As a similar estimation in the case of *A_c*, the rate constants *k_c* can be obtained from the *k_{obsd}* values at the saturation point of $[M^{m+}]_t$ against $[Q]_t$, being confirmed by experiments of varying salt concentrations. The Benesi–Hildebrand estimation based on the measurements of *k_{obsd}* at varying concentration of metal cation was also applied to obtain the *K_{QM^{m+}}* and *k_c*, when the couples of host and guest showed absorption change on the condition of $[M^{m+}]_t/[Q]_t \geq 10$.¹⁰

These treatments to determine *K_{QM^{m+}}* and *k_c* values were applied for the rather strong complexations of quinocrown ethers with di- and trivalent cations.

Alkali Metal and Ammonium Ion Catalyzed Reactions. A part of this study was reported as a communication; see ref 4l. We first carried out a systematic kinetic study under the same experimental conditions for the [4 + 2] cycloaddition of 15–21 membered quinocrown ethers **1a–d** and reference dimethoxyquinone **2** (0.167 mM) with a large excess of cyclopentadiene (16 mM) with or without 24 equiv excess of alkali metal and ammonium perchlorates (4.0 mM) in acetonitrile at 30 °C.¹¹

In the absence of metal salt, all quinones **1a–d** and **2** provided comparable rate constants *k_f* ranging from 4.6 to 5.3×10^{-2} M⁻¹ s⁻¹ irrespective of having cyclic or acyclic substituents (Table 1). However, the addition of metal salts brought about varying rate enhancements, reflecting selective cation binding abilities.¹² The most

**Figure 2.** Plot of $\ln(k_{obsd}/k_f)$ vs the alkali metal ion radius (Å), where *k_{obsd}* and *k_f* represent the rate constants for the reactions in the presence and absence of added alkali metal perchlorates (4.0 mM), respectively.

selective alkali metal ions responsible for the maximum rate were Na⁺ for **1a**, K⁺ for **1b** and **1d**, and Cs⁺ for **1c**, achieving accelerations of *k_{obsd}*/*k_f* by factors of 2.3–3.7. As to NH₄⁺, the maximum rate (*k_{obsd}*/*k_f* = 2.8) was attained for 18-membered crown ether **1b**. The reference dimethoxyquinone **2** showed no appreciable rate dependency on addition of metal salts; *k_{obsd}*/*k_f* = 1.0–1.1. These results indicate that the size-fitted complexation of a quinocrown ether with an alkali metal ion can promote the cycloaddition more effectively.

The overall kinetic features associated with the selective cation binding can be more explicitly visualized in the plot of $\ln(k_{obsd}/k_f)$ vs metal ion radius (Figure 2). These rate profiles for quinocrown ethers **1a–d** apparently reflect the selective rate enhancement of the cycloaddition by cation recognition. In crown ether chemistry, the size-fit concept is the most widely accepted and frequently referenced basic idea in explaining the relative cation selectivity of crown ethers with varying ring sizes.^{1,12–15} We would like to resort on this concept to interpret the selective rate-acceleration by monovalence cations.

Accordingly, 15-membered **1a** gave the peak top (*k_{obsd}*/*k_f* = 2.7) at Na⁺ (ion radius 0.95 Å) by analogy with the complexation of usual 15-crown-5 (cavity radius 0.86–

(8) (a) Leggett, D. J., Ed.; *Computational Methods for the Determination of Formation Constants*; Plenum: New York, 1985. (b) Connors, K. A. *Binding Constants*; Wiley: New York, 1987.

(9) Benesi, H.; Hildebrand, J. H. *J. Am. Chem. Soc.* **1949**, *71*, 2703.

(10) (a) Baker, D. S.; Gold, V.; Sghibartz, C. M. *J. Chem. Soc., Perkin Trans. 2* **1983**, 1121. (b) Raganathan, K. G.; Schneider, H.-J. *Angew. Chem., Int. Ed. Engl.* **1996**, *35*, 1219. (c) Molenveld, P.; Kapsabelis, S.; Engbersen, J. F. J.; Reinhoudt, D. N. *J. Am. Chem. Soc.* **1997**, *119*, 2948.

(11) Reactions of **1b** (1 mM) with 20 equiv excess of cyclopentadiene at 25 °C for 1 h in acetonitrile solution containing 4 mM of KClO₄ or Ba(ClO₄)₂ led to almost the quantitative formation of [4 + 2] *endo* adduct as confirmed by ¹H NMR spectroscopy.

(12) Jong, D. F. Reinhoudt, D. N. *Stability and Reactivity of Crown Ether Complexes*; Academic Press: New York, 1981.

(13) (a) Christensen, J. J.; Eatough, D. J.; Izatt, R. M. *Chem. Rev.* **1974**, *74*, 351. (b) Izatt, R. M.; Terry, R. E.; Nelson, D. P.; Chan, Y.; Eatough, D. J.; Bradshaw, J. S.; Hansen, L. D.; Christensen, J. J. *J. Am. Chem. Soc.* **1976**, *98*, 7626. (c) Lamb, J. D.; Izatt, R. M.; Swain, C. S.; Bradshaw, J. S.; Christensen, J. J. *J. Am. Chem. Soc.* **1980**, *102*, 479. (d) Bock, H.; Hierholzer, B.; Vogtle, F.; Hollmann, G. *Angew. Chem., Int. Ed. Engl.* **1984**, *23*, 57. (e) Togo, H.; Hashimoto, K.; Morihashi, K.; Kikuchi, O. *Bull. Chem. Soc. Jpn.* **1988**, *61*, 3026. (f) Inoue, Y.; Hakushi, T.; Liu, Y.; Tong, L.-H.; Hu, J.; Zhao, G.-D.; Huang, S.; Tian, B.-Z. *J. Phys. Chem.* **1988**, *92*, 2371. (g) Liu, Y.; Lu, T.-B.; Tan, M.-Y.; Hakushi, T.; Inoue, Y. *J. Phys. Chem.* **1993**, *97*, 4548. (h) Inoue, Y.; Hakushi, T.; Liu, Y.; Tong, L.-H. *J. Org. Chem.* **1993**, *58*, 5411.

(14) Izatt, R. M.; Christensen, J. J. *Synthetic Multidentate Macrocyclic Compounds*; Academic Press: New York, 1978.

(15) (a) Izatt, R. M.; Bradshaw, J. S.; Nielson, S. A.; Lamb, J. D.; Christensen, J. J. *Chem. Rev.* **1985**, *85*, 271. (b) Bajaj, A. V.; Poonia, N. S. *Coord. Chem. Rev.* **1988**, *87*, 55. (c) Izatt, R. M.; Pawlak, K.; Bradshaw, J. S.; Bruenig, R. L. *Chem. Rev.* **1991**, *91*, 1721.

1.1 Å).^{1,12–15} A more selective rate profile accompanied by the peak shift ($k_{\text{obsd}}/k_f = 3.7$) to K^+ (1.33 Å) was attained for 18-membered **1b**. The high K^+ binding ability of 18-crown-6 (cavity radius 1.3–1.6 Å) is well recognized.^{1,12–15} Here, of notice is that the quinobenzo-difused 18-membered **1d** showed a smaller rate-acceleration especially for larger cations K^+ to Cs^+ with the peak at K^+ ($k_{\text{obsd}}/k_f = 2.3$). This can be explained by the restricted freedom of crown ring fused by the conformationally constrained aromatic ring. It is well-known that the benzocrown ethers have reduced cation binding abilities as compared with the parent crown ethers with the same ring size.^{15,16} As found for 21-membered **1c**, one more oxyethylene unit enlargement produced rather poor acceleration accompanied by a small peak at Li^+ ($k_{\text{obsd}}/k_f = 1.7$), although the maximum rate was still observed at the cavity-fitted cation Cs^+ ($k_{\text{obsd}}/k_f = 2.6$).

As unambiguous evidence for the selective alkali-metal cation binding of quinocrown ethers, we can rely on the ESI-MS measurements, which exhibited essentially the similar binding behaviors as the above rate profiles.¹⁷

Alkaline-Earth Metal Ion Catalyzed Reactions. Effects of Binding Constants, Geometry, and Valence of Complexes on Rates. What determines the magnitude of rate-enhancement? The possible three main factors we need to consider are (1) binding constants, (2) coordination-geometry, and (3) metal valence of the complex formed. Herein after in this section, we converge on the clarification of the origin of the cation recognized acceleration of the present Diels–Alder reaction. Hence, we examined $K_{\text{QM}^{2+}}$ and k_c values from the concentration-(salts)-dependent kinetic study for alkaline-earth metal and Sc^{3+} salts (vide supra).

As shown in Table 2, the alkaline-earth metal ions caused a larger rate-acceleration for quinocrown ethers **1a–d** ($k_c/k_f = 5–162$) than the monovalent alkali metal ions ($k_{\text{obsd}}/k_f = 1.3–3.7$, see Table 1). However, the reference **2** was negligibly affected by addition of even 24 equiv excess of these divalent metal ions. We first compared the quantities of k_c/k_f with the binding constants $K_{\text{QM}^{2+}}$ in order to know whether the reaction rates increase with increasing stability of QM^{2+} complex in solution. A survey of Table 2 showed that, except for **1d**, the largest k_c/k_f and $K_{\text{QM}^{2+}}$ values were attained by different ions: Ca^{2+} and Sr^{2+} for **1a**, Sr^{2+} and Ba^{2+} for **1b**, Mg^{2+} and Ba^{2+} for **1c**, respectively. These findings apparently indicate that the stability of QM^{2+} complexes is not directly correlated to the HOMO energy reduction of quinone function. The details of each quinocrown ether will be described below.

Quino[15]crown-5 (1a). The most stable QM^{2+} complex of 15-membered **1a**, as assessed by $K_{\text{1a}\cdot\text{M}^{2+}}$, is not with the size-fitted Ca^{2+} (0.99 Å) but with the next larger Sr^{2+} (1.13 Å) ($K_{\text{1a}\cdot\text{Sr}^{2+}}/K_{\text{1a}\cdot\text{Ca}^{2+}} = 4.10$) (Table 2). Izatt et al. also reported a similar deviation of the binding constants from the hole-size-selectivity for 15-crown-5 with the larger divalent cations such as Sr^{2+} or Ba^{2+} (1.35 Å).¹⁸ In general, 15-membered crown ethers prefer to

Table 2. Alkaline-Earth Metal Ion Catalyzed Diels–Alder Reactions of Quinones 1a–d and 2 with Cyclopentadiene in MeCN at 30 °C^a

quinone (Q)	additive ^b	10 $k_c/M^{-1} s^{-1}$	log $K_{\text{QM}^{2+}}$	k_c/k_f^d
1a	Mg^{2+}	4.39	2.65	8.4
	Ca^{2+}	6.16	4.11	12
	Sr^{2+}	5.11	4.72	9.8
	Ba^{2+}	3.23	4.62	6.2
1b	Mg^{2+}	^e	^e	–
	Ca^{2+}	3.36	5.28	7.3
	Sr^{2+}	5.63	5.33	12
	Ba^{2+}	4.71	6.33	10
1c	Mg^{2+}	77.1	2.11	162
	Ca^{2+}	8.08	4.93	17
	Sr^{2+}	2.51	5.02	5.3
	Ba^{2+}	3.48	5.64	7.3
1d	Mg^{2+}	^e	^e	–
	Ca^{2+}	3.82	4.03	7.2
	Sr^{2+}	3.71	4.23	7.5
	Ba^{2+}	4.08	5.01	7.7
	2	Mg^{2+}	(0.582)	^e
	Ca^{2+}	(0.593)	^e	(1.1)
	Sr^{2+}	(0.540)	^e	(1.0)
	Ba^{2+}	(0.565)	^e	(1.1)

^a Kinetic reactions were carried out under pseudo-first-order conditions by using ca. 10–100 equiv excess of cyclopentadiene (2.0–16.0 mM) with respect to quinones **1** and **2** (0.167 mM).

^b Counteranion perchlorate (ClO_4^-) is omitted. ^c The k_c values were obtained from the k_{obsd} values at the saturation point of $[\text{Q}\cdot\text{M}^{2+}]$. The values in parentheses are k_{obsd} for the cycloaddition of **2** (0.167 mM) in the presence of 24 equiv excess of alkaline-earth metal perchlorates (4.0 mM). ^d The values in parentheses are the values of k_{obsd}/k_f . For the k_f values, see Table 1. ^e No applicable absorption change and rate-acceleration to calculate log $K_{\text{Q}\cdot\text{M}^{2+}}$ and k_c were observed.

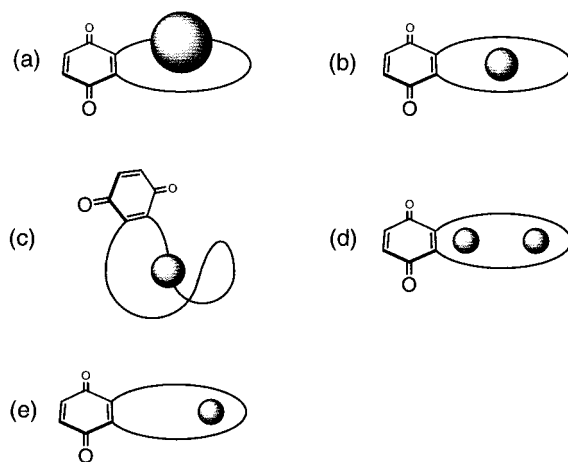


Figure 3. Schematic representation showing stoichiometry of crown ether– M^{m+} complexes and the conformation in the solution: (a) perching, (b) ion-in-the-hole (nesting), (c) wrapping, (d) dicationic-dinuclear, (e) hanging.

form “perching” complexes with the larger divalent cations as a consequence of a critical balance between the entropic and enthalpic factors (Figure 3a).¹⁹

The salt concentration-dependent kinetic profiles for **1a** explicitly show the unconformable relationship between k_{obsd} and $K_{\text{1a}\cdot\text{M}^{2+}}$ (Figure 4a). Up to ca. 1 equiv of $[\text{M}(\text{ClO}_4)_2]$, the k_{obsd} increased in the order of $\text{Sr}^{2+} > \text{Ba}^{2+} > \text{Ca}^{2+} > \text{Mg}^{2+}$ in conformity with the $K_{\text{1a}\cdot\text{M}^{2+}}$ values (Table 2). However, as the excess metal salts were increasingly added, the Ca^{2+} line intersected the Ba^{2+} and then the Sr^{2+} line and then rose over their saturated values k_c . This figure simply implies that the most effective rate-enhancement is achieved by the size-fitted Ca^{2+} complex rather than by the perching Sr^{2+} or Ba^{2+}

(16) (a) Inoue, Y.; Amano, F.; Okada, N.; Inada, H.; Ouchi, M.; Tai, A.; Hakushi, T.; Liu, Y.; Tong, L.-H. *J. Chem. Soc., Perkin Trans. 2* **1990**, 1239. (b) Liu, Y.; Tong, L.-H.; Inoue, Y.; Hakushi, T. *J. Chem. Soc., Perkin Trans. 2* **1990**, 1247. (c) Inoue, Y.; Nakagawa, K.; Hakushi, T. *J. Chem. Soc., Dalton Trans.* **1993**, 2279.

(17) Tsuda, A.; Moriwaki, H.; Oshima, T. *J. Chem. Soc., Perkin 2* **1999**, 1235.

(18) Lamb, J. D.; Izatt, R. M.; Swain, C. S.; Christensen, J. J. *J. Am. Chem. Soc.* **1980**, 102, 475.

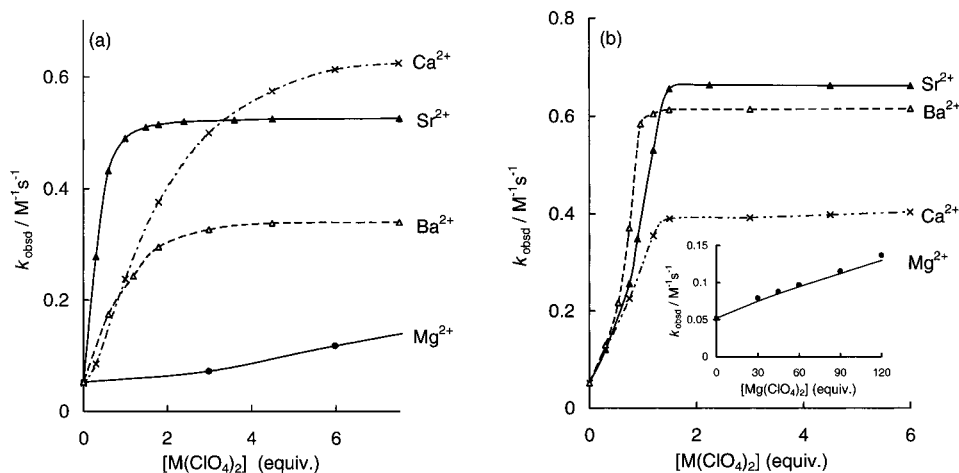


Figure 4. Dependence of k_{obsd} on concentration of $\text{M}(\text{ClO}_4)_2$ for Diels–Alder reaction of (a) quino[15]crown-5 **1a** (0.167 mM), (b) quino[18]crown-6 **1b** (0.167 mM) with cyclopentadiene (16 mM) in MeCN at 303 K (M = Mg, Ca, Sr, Ba). The k_{obsd} are plotted against the molar equivalents of added salt.

one with the larger $K_{\text{QM}^{2+}}$ values. Namely, the size-fitted Ca^{2+} can exert the most effective inductive and/or resonance electron withdrawal on the quinone function by way of the coordinating oxygen atoms. Such electronic effects would be much more intensified as the metal ion is located as close as possible to the quinone-conjunct oxygen atoms such as in the case of size-fitted “ion-in-the hole” complex for Ca^{2+} ion.^{12–15} Indeed, the k_c/k_f values decreased in the order $\text{Ca}^{2+} > \text{Sr}^{2+} > \text{Ba}^{2+}$ with the increasing deviation from the size-fitness. Also, it is interesting that the **1a**· Mg^{2+} complex, which most loosely binds Mg^{2+} (0.65 Å), gave a 1.4-fold larger k_c/k_f value than the typical “perching” complex **1a**· Ba^{2+} irrespective of large difference in binding constants ($K_{\text{1a} \cdot \text{Mg}^{2+}}/K_{\text{1a} \cdot \text{Ba}^{2+}} = 0.01$). This phenomenon strongly suggests that the rate-acceleration is actually not primarily dependent on the whole stability of the complex but on the efficiency with which the guest cation can exert the positive charge on the quinone function. Engberts et al. have also reported the absence of a correlation between rate effects and equilibrium constants in the Lewis acid-catalyzed Diels–Alder reactions of the bidentate dienophile 3-phenyl-1-(2-pyridyl)-2-propen-1-ones and cyclopentadiene in water.²⁰

Quino[18]crown-6 (1b) and Quinobenzo[18]crown-6 (1d). The 18-membered **1b** exhibited the largest k_c not for size-fitted Ba^{2+} but for rather smaller Sr^{2+} irrespective of having a 10-fold larger $K_{\text{1b} \cdot \text{M}^{2+}}$ for Ba^{2+} than for Sr^{2+} (Table 2). As seen in Figure 4b, until the kinetic saturation, the k_{obsd} increased with the increase of salt concentrations, in harmony with the increasing order of $K_{\text{1b} \cdot \text{M}^{2+}}$; $\text{Ba}^{2+} > \text{Sr}^{2+} > \text{Ca}^{2+} \gg \text{Mg}^{2+}$. However, upon further addition of metal salts, the Sr^{2+} line reached the maximum saturation k_c over the Ba^{2+} line. This embarrassing situation may also be understandable on the basis of the above-mentioned criterion for the efficient cation-induced rate-acceleration. That is, the bound Sr^{2+} is thought to come close to the quinone function as compared with the size-fitted Ba^{2+} possibly because of adopting the wrap-

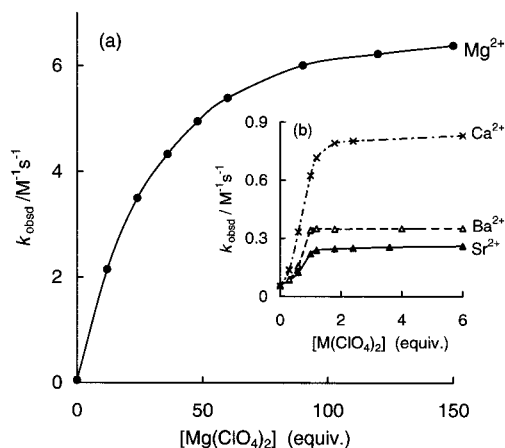


Figure 5. Dependence of k_{obsd} on concentration of (a) $\text{Mg}(\text{ClO}_4)_2$ and (b) $\text{M}(\text{ClO}_4)_2$ (M = Ca, Sr, Ba) for Diels–Alder reaction of quino[21]crown-7 **1c** (0.167 mM) with cyclopentadiene (4.0–16 mM) in MeCN at 303 K. The k_{obsd} are plotted against the molar equivalents of added salts.

ping-type conformation of crown ring (Figure 3c). In addition, the comparable large $K_{\text{1b} \cdot \text{Ca}^{2+}}$ value for the more smaller Ca^{2+} can be taken as further evidence for such three-dimensional complexation.

A comparison with additionally benzene-fused **1d** revealed the importance of the conformational freedom of the crown ring for efficient cation complexation. It is well-known that the fusion of the benzene ring on the macrocyclic ring diminishes its ability to accommodate cations mainly due to the reduction in flexibility of the ring as well as the resonating electron-withdrawal of benzene nucleus.¹⁶ Indeed, **1d** provided about one logarithmic unit smaller $K_{\text{1d} \cdot \text{M}^{2+}}$ values for the respective ions as compared with the parent **1b**. Furthermore, **1d** gave slightly declined k_c/k_f values and a poor ion-selectivity against Ca^{2+} to Ba^{2+} .

Quino[21]crown-7 (1c). The 21-membered **1c** has the most flexible crown ring, and its planar cavity size is far more larger than required for Ba^{2+} . Therefore, the size-fit-concept is no longer applicable to assess the magnitude of rate-acceleration as seen in Table 2 and Figure 5. For instance, Mg^{2+} brought about an abnormally high rate-enhancement (162-fold), irrespective of the lowest log $K_{\text{1c} \cdot \text{Mg}^{2+}}$ value of 2.11. It is well-known that the usual 21-

(19) (a) Inoue, Y.; Ouchi, M.; Hosoyama, K.; Hakushi, T.; Liu, Y.; Takeda, Y. *J. Chem. Soc., Dalton Trans.* **1991**, 1291. (b) Inoue, Y.; Liu, Y.; Tong, L.-H.; Ouchi, M.; Hakushi, T. *J. Chem. Soc., Perkin Trans. 2* **1993**, 1947.

(20) Otto, S.; Bertoncin, F.; Engberts, J. B. F. N. *J. Am. Chem. Soc.* **1996**, *118*, 7702.

membered crown ethers have very poor affinity for Mg^{2+} in various solvents.^{13–15} These findings suggest that one of the quinone carbonyl groups may also take part in the complexation of Mg^{2+} by constructing a three-dimensional cavity with a highly flexible twisted crown ring like that in lariat crown ethers.²¹ In fact, the ^1H NMR spectra of **1c** (0.25 mM) in CD_3CN at 30 °C revealed that the quinone vinyl protons ($\delta = 6.58$ ppm) were considerably shifted toward lower magnetic field by 0.22 ppm for **1c**· Mg^{2+} complex ($\text{Mg}(\text{ClO}_4)_2 = 75.0$ mM), but only 0.04 ppm for the **1c**· Ba^{2+} complex ($\text{Ba}(\text{ClO}_4)_2 = 5.0$ mM) (Supporting Information). Furthermore, all the signals of **1c**· Mg^{2+} were relatively broadened as compared with those of the **1c**· Ba^{2+} as well as **1c**. These observations imply some constrained geometrical transformation of crown ring probably caused by the additional coordination of quinone carbonyl group to the incorporated Mg^{2+} ion. Incidentally, we have observed a notable rate-acceleration in a similar Diels–Alder reaction of mono-substituted noncyclic triglymed quinone, in which the addition of Mg^{2+} caused 390-fold increment ($\log K_{\text{Q} \cdot \text{Mg}^{2+}} = 0.79$).²² The lariat oligoethylene glycol chain can probably incorporate Mg^{2+} with the aid of a quinone oxygen atom.

Herein, one can consider the possibility that this abnormal rate-enhancement may be due to the formation of a multinuclear complex, judging from the 21-membered crown cavity and Mg^{2+} cation size (Figure 3d).²³ However, this possibility seems to be ruled out by a Hill-plot of kinetic data.²⁴ The 1:1 stoichiometry of **1c** with Mg^{2+} was confirmed by the plot of $\log([\mathbf{1c} \cdot \text{Mg}^{2+}]/[\mathbf{1c}])$ vs $\log[\text{Mg}^{2+}]$ at a constant crown ether concentration based on the kinetic data of Figure 5, where $[\mathbf{1c} \cdot \text{Mg}^{2+}]$, $[\mathbf{1c}]$, and $[\text{Mg}^{2+}]$ are the complex, crown, and metal concentrations, respectively, which gives a line with a slope of 1 within experimental error.

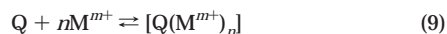
For the next combination of **1c** with Ca^{2+} , a 17-fold acceleration and the relatively large $K_{\mathbf{1c} \cdot \text{Ca}^{2+}}$ were observed. The stoichiometry of the 1:1 ion-crown complex was also deduced from the Job plot experiment by the

(21) (a) Echegoyen, L.; Kaifer, A.; Durst, H.; Schultz, R. A.; Dishong, D. M.; Goli, D. M.; Gokel, G. W. *J. Am. Chem. Soc.* **1984**, *106*, 5100. (b) Schultz, R. A.; White, B. D.; Dishong, D. M.; Arnold, D. K.; Gokel, G. W. *J. Am. Chem. Soc.* **1985**, *107*, 6659. (c) Gustowski, D. A.; Delgado, M.; Gotto, V. J.; Echegoyen, L.; Gokel, G. W. *Tetrahedron Lett.* **1986**, *27*, 3487. (d) Miller, S. R.; Gustowski, D. A.; Chen, Z.-H.; Gokel, G. W.; Echegoyen, L.; Kaifer, A. E. *Anal. Chem.* **1988**, *60*, 2021.

(22) The study on the “effects of cation recognition on kinetics of Diels–Alder reaction of open chain oligoether quinones with cyclopentadiene” will be reported as a next paper.

(23) (a) Mercer, M.; Truter, M. R. *J. C. S. Dalton.* **1973**, 2469. (b) Hughes, D. L. *J. C. S. Dalton.* **1975**, 2374. (c) Inoue, Y.; Liu, Y.; Amano, F.; Ouchi, M.; Tai, A.; Hakushi, T. *J. Chem. Soc., Dalton Trans.* **1988**, 2735.

(24) The overall equilibrium between quinocrown ether (Q) and cation (M^{m+}) in solution is expressed in the general form of eq 9, where the ratio 1:n denotes the crown:cation stoichiometry. The equilibrium constant $K_{\text{QM}^{m+}}$ is given by eq 10. Modification of eq 10 leads to eq 11 with $[\text{M}^{m+}]$ as a variant. The binding constant $K_{\text{QM}^{m+}}$ and the complex stoichiometry can be determined by the intercept and slope, respectively, of eq 11.



$$K_{\text{QM}^{m+}} = \frac{[\text{Q}(\text{M}^{m+})_n]}{[\text{Q}][\text{M}^{m+}]^n} \quad (10)$$

$$\log([\text{Q}(\text{M}^{m+})_n]/[\text{Q}]) = n \log[\text{M}^{m+}] + \log K_{\text{QM}^{m+}} \quad (11)$$

$$[\text{Q}] = [\text{Q}]_t - [\text{Q}(\text{M}^{m+})_n]$$

$$[\text{M}^{m+}] = [\text{M}^{m+}]_t - [\text{Q}(\text{M}^{m+})_n]$$

Table 3. Scandium Ion Catalyzed Diels–Alder Reactions of Quinones **1a–d** and **2** with Cyclopentadiene in MeCN at 30 °C^a

quinone (Q)	additive ^b	$k_c/M^{-1} \text{ s}^{-1}$	$\log K_{\text{Q} \cdot \text{Sc}^{3+}}$	k_c/k_f^d
1a	Sc^{3+}	96.2 ^e	2.40	2021
1b	Sc^{3+}	46.5 ^e	2.74	977
1c	Sc^{3+}	4.92 ^f	4.84	103
1d	Sc^{3+}	175 ^e	2.13	3676
2	Sc^{3+}	(1.46)	^g	(27.3)

^a Kinetic reactions were carried out under *pseudo*-first-order conditions by using ca. 10–100 equiv excess of cyclopentadiene (2.0–16.0 mM) with respect to quinones **1** (0.167 mM). ^b Counteranion triflate (OTf^-) is omitted. ^c The value in parentheses is k_{obsd} for the cycloaddition of **2** (0.167 mM) in the presence of 24 equiv excess of $\text{Sc}(\text{OTf})_3$ (4.0 mM). ^d The value in parentheses is the value of k_{obsd}/k_f . For the k_f values, see Table 1. ^e Estimated from the Benesi–Hildebrand analysis. ^f Obtained from the k_{obsd} at the saturation point of $[\mathbf{1c} \cdot \text{Sc}^{3+}]$. ^g No applicable absorption change to calculate $\log K_{\text{Q} \cdot \text{Sc}^{3+}}$ was observed.

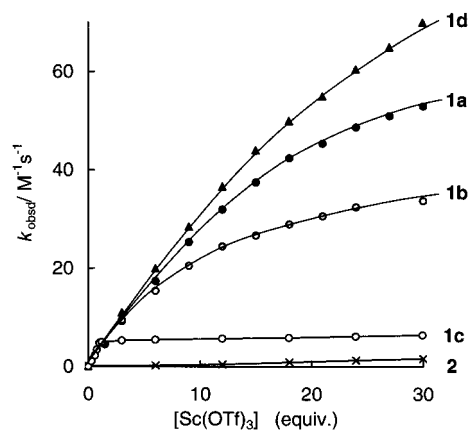


Figure 6. Dependence of k_{obsd} on concentration of $\text{Sc}(\text{OTf})_3$ for Diels–Alder reaction of quinocrown ethers **1a–d** (0.167 mM) with cyclopentadiene (2.0 mM) in MeCN at 30 °C. The k_{obsd} are plotted against the molar equivalents of added salts.

UV–visible spectroscopic procedure.²⁵ A plot of complex concentration versus $[\text{Ca}(\text{ClO}_4)_2]/([\mathbf{1c}] + [\text{Ca}(\text{ClO}_4)_2])$ shows a maximum at 0.5. The appreciably large $K_{\text{QM}^{2+}}$ and k_c/k_f values of the **1c**· Ca^{2+} complex may be accounted for by the wrapping conformation.²⁶ On the other hand, the complexes **1c**· Sr^{2+} and **1c**· Ba^{2+} provided considerably reduced k_c/k_f ($=5.3 - 7.3$) despite comparably large $K_{\mathbf{1c} \cdot \text{Sr}^{2+}}$ values.

Sc^{3+} Ion Catalyzed Reactions. As shown in Table 3 and Figure 6, the more astonishing rate-enhancements were caused by trivalent Sc^{3+} for 15–21-membered quinocrown ethers **1a–d** ($k_c/k_f = 103$ –3676), although the reference **2** suffered a considerably diminished effect ($k_{\text{obsd}}/k_f = 27.3$) on 24 equiv addition of $\text{Sc}(\text{OTf})_3$. It is also noted that the increasing order of k_c/k_f values (**1d** > **1a** > **1b** > **1c**) is quite opposite to that of $K_{\text{Q} \cdot \text{Sc}^{3+}}$ (**1c** > **1b** > **1a** > **1d**).

All quinocrown ethers **1a–d** do not efficiently form size-fitted ion-in-the-hole complexes with the tiny Sc^{3+} (0.81 Å). Therefore, the increasing $K_{\text{Q} \cdot \text{Sc}^{3+}}$ value in going from **1a** to **1c** is unambiguously ascribed to the increasing flexibility of the crown ring which is of great advantage to bind the charge-condensed high valence Sc^{3+} by *wrapping* or *hanging* complexation (Figure 3c and 3e).

(25) Job, A. *Ann. Chim. (Paris)* **1928**, *9*, 113.

(26) (a) Bush, M. A.; Truter, M. R. *J. Chem. Soc., Trans. Perkin 2* **1972**, 345. (b) Live, D.; Chan, S. I. *J. Am. Chem. Soc.* **1976**, *98*, 3769.

In fact, the 21-membered **1c** has about a two log unit larger $K_{Q\cdot Sc^{3+}}$ value than others, while the stiffness of benzene-fused 18-membered **1d** leads to the smallest $K_{Q\cdot Sc^{3+}}$. Accordingly, the opposite relationship between the $K_{Q\cdot Sc^{3+}}$ and the k_c/k_f values can be explained by considering the coordination geometry of Sc^{3+} complexes.

Since the magnitudes of rate-enhancement are directly correlated with the electron-withdrawal of the guest cations, it can be said that the decreasing order of k_c/k_f values from **1a** to **1c** is confidently due to the increasing distance between the guest ion and quinone function as mentioned above. The tiny Sc^{3+} is necessarily located more closely to the quinone function in the 15-membered **1a**, causing ca. 2- and 20-times larger rate-acceleration than **1b** and **1c**. The smallest k_c/k_f value for 21-membered **1c** is suggestive of the highly developed *hanging* complexation of Sc^{3+} . In fact, the hanging structure is confirmed by the 1H NMR spectrum of **1c** (0.25 mM) with 4 equiv excess of $Sc(OTf)_3$ in CD_3CN , which exhibited a larger downfield shift for the remote oxyethylene protons (0.6–0.8 ppm) as compared with the quinone-adjacent oxyethylene protons (0.25–0.6 ppm).

It is interesting that benzene-fused **1d** enjoyed the maximum rate-acceleration of 3700-fold (ca. 4-times larger than the parent **1b**) despite the lowest $K_{Q\cdot Sc^{3+}}$ value. The smallest $K_{Q\cdot Sc^{3+}}$ can be due to the intrinsic stiffness of **1d** as compared with **1b**. However, the large rate-acceleration is better explained by the enhanced electron-withdrawal of Sc^{3+} . Considering that OTf^- is more bulky than ClO_4^- and that the constrained benzene ring exerts the significant steric effects on the crown ring, Sc^{3+} should be located closer to the quinone function. As a result, these findings indicate that the geometrical features of the complexes play a crucial role in the rate-acceleration.

Conclusions

We have found that Diels–Alder reactions of 15–21 membered-ring quinocrown ethers **1a–d** with cyclopentadiene are accelerated up to maximal 3700 times by the addition of alkali, alkaline-earth, and scandium metal salts, reflecting characteristic cation recognition of respective crown rings. The rate-acceleration stems from the cation-induced reduction of LUMO energy of quinone suitable for the FMO interaction with the HOMO of cyclopentadiene. The magnitude of rate-enhancement is governed by the three main factors. (1) Binding constants. The binding constants ($K_{QM^{m+}}$) represent the thermodynamic features of complexation of crowns with guest cations, that is, the population of complex species. Thus, the $K_{QM^{m+}}$ values dominantly affect the rates until the saturated kinetics is attained. In general, the $K_{QM^{m+}}$ does not correlate with the saturated k_c value according to the next two factors. (2) Coordination geometry of complex. Since the LUMO energy of the quinone function is dependent on the distance between the guest cation and quinone moiety, the following three geometrical features play an important role in the selective rate-acceleration: (I) the *size-fitted complex* can realize the favorable ion–dipole interaction to cause the effective electron-withdrawal from the quinone moiety, (II) the *perching complex* will diminish such electronic effects because of the elongated interaction, (III) the largely flexible crowns can bind smaller multivalence cations close to or remote from

the quinone function by adopting a *wrapping* or *hanging* complexation. (3) Valence of cation. Despite the variation of coordination geometry as well as the ion sizes and crown ring sizes, the rates significantly increase with increasing valence of the guest cations (alkali metal (M^+) < alkaline-earth metal (M^{2+}) < Sc^{3+} ion) because of the intensified electrostatic interaction with crown rings.

Experimental Section

Melting points were measured with a Yanagimoto melting-point apparatus and were uncorrected. NMR spectra were recorded on a JEOL EX-270 spectrometer using trimethylsilane(TMS) as an internal standard. IR spectra were recorded on a JASCO FT/IR-410 spectrometer. Mass spectra were obtained with a JEOL JMS-DX303 spectrometer and a SHIMAZU GCMS-QP200A gas chromatograph mass spectrometer. UV–visible spectra were recorded on a JASCO V-550 spectrometer equipped with a PELTIER EHC-447 thermostated cell-holder.

Materials. All the metal perchlorates and triflate were of commercial origin and were used without further purification. Spectrally pure acetonitrile (water <0.03%, Nakarai Chemical Co., Ltd.) was used for the kinetic and spectroscopic solutions. Cyclopentadiene was obtained from its dimer by distillation just before use. The quinocrowns **1a** and **1b** were prepared according to the published methods, and their adducts with cyclopentadiene in Diels–Alder reactions were also reported.⁶ The syntheses of **1c** and **1d** were described elsewhere.¹⁷

Kinetic Measurements. The general kinetic experiments were performed under *pseudo*-first-order conditions in acetonitrile solution containing a quinone (0.167 mM) and a large excess of cyclopentadiene (2.0 – 16.0 mM) with or without addition of alkali, alkaline-earth metal, ammonium perchlorates, and scandium triflate at 30 °C. The rates of reaction were determined by monitoring the disappearance of the absorption due to the quinones **1a–d**, and **2** at $\lambda_{max} = 391–399$ nm.⁷ The rates obeyed pseudo-first-order kinetics up to at least two half-lives, and the second-order rate constants were obtained by dividing the observed first-order rate constants with the corrected concentration of cyclopentadiene on the consumption of the half amount of quinone.

Cycloadduct of 1c. A 50-mL round-bottled flask was charged with a **1c** (50 mg, 0.13 mmol) in acetonitrile (20 mL). The reaction vessel was covered with aluminum foil. Cyclopentadiene (10 equiv excess) was added in one portion. After the mixture had been stirred for 2 h, the solvent was removed under the reduced pressure. The product was finally separated by flash chromatography over a silica gel (Wakogel C-400) column. Elution with $CHCl_3$ gave the *endo*-cycloadduct of **1c** in 92% yield (54 mg); 1H NMR (270 MHz, $CDCl_3$) δ 1.25 (s, 1H), 1.43 (s, 1H), 3.18–3.19 (t, $J = 1.8$ Hz, 2H), 3.50 (m, 2H), 3.65 (s, 8H), 3.67 (s, 8H) and 3.76–3.79 (m, 4H), 4.35–4.39 (m, 4H), 6.06 (t, $J = 1.8$ Hz, 2H); IR (KBr) 2920, 1662, 1616, 1590, 1458, 1349, 1280, 1109, 949, 841, and 716 cm^{-1} ; MS (EI) m/e 452 (M^+ , 15%), 388 (59), 166 (100), 138 (70), 73 (62), 45 (95). Anal. Calcd for $C_{23}H_{32}O_9$: C, 61.05; H, 7.13. Found: C, 61.15; H, 7.08.

Cycloadduct of 1d. Similar procedure for **1d** with cyclopentadiene gave the corresponding *endo*-cycloadduct in 94% (54 mg); brown oil; 1H NMR (270 MHz, $CDCl_3$) δ 1.25 (s, 1H), 1.43 (s, 1H), 3.09–3.31 (t, $J = 1.8$ Hz, 2H), 3.44 (s, 2H), 3.84–3.90 (m, 8H), 4.13–4.36 (m, 4H), 4.34–4.42 (m, 2H), 4.45–4.58 (m, 2H), 6.03–6.04 (t, $J = 1.8$ Hz, 2H) 6.84–6.93 (m, 4H); IR (KBr) 3062, 2933, 2873, 1663, 1590, 1505, 1452, 1336, 1256, 1129, 1062, 934, and 747 cm^{-1} ; MS (EI) m/e 456 (M^+ , 10%), 390 (64), 136 (100), 121 (60). Anal. Calcd for $C_{25}H_{28}O_8$: C, 65.78; H, 6.18. Found: C, 65.63; H, 6.31.

Acknowledgment. This work was supported by a Grant-in-Aid for Scientific Research on Priority Areas

(No.10650849) from the Ministry of Education, Science, and Culture of the Japanese Government. We are grateful to Professor Dr. Yoshihisa Inoue (Osaka University) for helpful discussion.

Supporting Information Available: ^1H NMR spectra of **1c**, **1c**· Mg^{2+} , and **1c**· Ba^{2+} in CD_3CN at 30 °C. This material is available free of charge via the Internet at <http://pubs.acs.org>. JO010991E